White Rose Research Online

eprints@whiterose.ac.uk
https://eprints.whiterose.ac.uk
Universities of Leeds, Sheffield and York

Deposited via The University of Leeds.

White Rose Research Online URL for this paper:
https://eprints.whiterose.ac.uk/id/eprint/85463/

Version: Accepted Version

Article:
Lea-Langton, AR, Baeza-Romero, MT, Boman, GV et al. (2015) A study of smoke formation from wood combustion. Fuel Processing Technology, 137. 327 - 332. ISSN: 0378-3820

https://doi.org/10.1016/j.fuproc.2015.03.020

© 2015, Elsevier. Licensed under the Creative Commons Attribution-NonCommercial-NoDerivatives 4.0 International http://creativecommons.org/licenses/by-nc-nd/4.0/

Reuse
Items deposited in White Rose Research Online are protected by copyright, with all rights reserved unless indicated otherwise. They may be downloaded and/or printed for private study, or other acts as permitted by national copyright laws. The publisher or other rights holders may allow further reproduction and re-use of the full text version. This is indicated by the licence information on the White Rose Research Online record for the item.

Takedown
If you consider content in White Rose Research Online to be in breach of UK law, please notify us by emailing eprints@whiterose.ac.uk including the URL of the record and the reason for the withdrawal request.

UNIVERSITY OF LEEDS
University of Sheffield
UNIVERSITY of York

A Study of Smoke Formation from Wood Combustion.

A.R.Lea-Langton[1], M.T.Baeza-Romero[2], G.V.Boman[3], B. Brooks[3], A.J.M.Wilson[3], F.Atika[1] K.D.Bartle[1] J.M.Jones[1], A.Williams[1],

1 Energy Research Institute, University of Leeds, Leeds, LS2 9JT, UK.

2 Escuela de Ingeniería Industrial de Toledo, Universidad de Castilla la Mancha, 45071, Spain
3 School of Earth and Environment, University of Leeds, Leeds, LS2 9JT, UK.

Communicating author: Dr A R Lea-Langton: A.R.Lea-Langton@leeds.ac.uk

Abstract

Aerosol time of flight mass spectrometry (ATOFMS) was used to analyse the particles emitted during the flaming and smouldering phases of the combustion of samples of hard and soft woods. Eugenol and furfural were also burned and using results from previous work of the authors, they have been shown to be useful proxies for initial wood combustion products. The ratios of elementary carbon to total carbon in the particles were similar for both the woods and for eugenol. The ATOFMS spectra of most of the particles were consistent with the presence of soot precursor constituents along with oxygen containing fragments. Most particle diameters were less than 2.5 μm, with the greatest concentration<0.12μm

Keywords: wood, combustion, particulate matter

1. Introduction.

Solid biomass is a renewable fuel that is burned globally and particularly in developing countries. This use declined during the era of fossil fuels but the need for a low carbon energy source has resulted in a revival in its use. The difficulty is that in certain circumstances e.g. in small domestic stoves particularly of the type used in developing countries, biomass can form smoke which is both a health hazard [1] and an environmental problem through its influence on climate change [2]. The health hazards arise from the small particles (< 2.5μm) present in the smoke which are accompanied by toxic aromatic hydrocarbons such as phenols as well as polyaromatic hydrocarbons and related compounds which are carcinogenic [1]. The climate change problems arise from the same group of pollutants but on a global scale. This is because the carbon particles termed black carbon (BC) together with the organic compounds (OC) are climate forcing agents approximately being responsible for 25% of the total climate change [2]. Black carbon warms the Earth by absorbing heat in the atmosphere and by reducing albedo, the ability to reflect sunlight, when deposited on snow and ice. OC have a negative effect so the balance of the BC/OC influence is very important [2]. In addition to the anthropogenic combustion of biomass, wild fires are also another major source of smoke.

The general mechanism of biomass combustion has been extensively studied over a number of years [3-10], but recently much attention has been directed to the emission of fine particles, that is below 2.5μm. In previous work, we considered that the cellulose and lignin components can be treated separately in relation to their emissions [4,5]. Cellulose decomposes largely to CO and H_2 together with other small molecules, while lignin

decomposes to more complex aromatic products. Using proxy compounds for wood combustion (eugenol and furfural) we previously investigated [11] the mechanism of smoke formation and concluded that the cellulose compounds can form smoke via hydrogen abstraction/ carbon addition (HACA), and that the lignin products form smoke through an aromatic species mechanism. In this paper, we report an investigation using aerosol time-of-flight mass spectrometry (ATOFMS, TSI 3800-100) of the size and composition of particles emitted during the combustion of real wood: softwood (pine and spruce) and hardwood (short-rotation coppice willow). Comparisons are made between results obtained for the wood samples and those for the proxies, and between those from two modes of combustion, flaming and smouldering conditions. An additional factor is the release of potassium from wood combustion [6,12,13] which can have a significant influence on the nature of the soot emitted from wood flames. In consequence this is important in determining the ratio of elementary to total carbon (EC/TC) ratio for the particular biomass.

For comparative purposes, additional information on smoke formation from the combustion of eugenol and furfural is presented here. We have previously shown that smoke from eugenol can be attributed to the lignin components of biomass [11] and is a major contributor to smoke formation. Furfural is produced largely by the cellulose and has been shown to produce less soot.

2. Experimental.

Samples of wood chips were burned on a 100mm diameter stainless steel mesh (5mmx5mm hole) supported 50mm high by a stand in a vertical 130mm diameter quartz tube. The role of this tube which was 300mm high was to contain and steady the flame. A flow of clean combustion air was introduced uniformly through holes at the bottom of the quartz tube at a flow rate of approximately 14 Lmin-1. The combustion products were sampled directed by a glass funnel located over the top of the quartz tube and passed to the ATOFMS inlet by a short (500mm) teflon tube. The general arrangement is shown in Fig, 1.

Figure 1 here

Samples of a softwood (pine/spruce mix) and hardwood (short-rotation coppice willow) chips were used. The former contained 800 ppm potassium and 0.3 wt% ash and the hardwood contained 4000 ppm potassium and 4 wt% ash. 5g samples of chips (about 1cm long and 0.5 cm diameter) were burned on the wire mesh. The wood was ignited with a butane torch for

approximately 25s and when fully ignited the combustion products were sampled. Separate sets of runs were carried out with the wood either flaming or smouldering conditions. The air flow was kept constant so that combustion takes place with excess air available, overall the ratio of excess air to that of the combustion products was a factor of three.. However, the air entrained into the flame zone would be greater during the flaming stage compared with the smouldering phase because of the more rapid combustion.

The ATOFMS (Model 3800-100 from TSI Inc.) provides information on the aerodynamic size and chemical composition of particles in the size range 100-3000 nm in diameter. Particles smaller than100 nm can be sampled and analysed (mass spectra can be obtained) with this set up, but with very low efficiency since the transmission of the aerodynamic lens decreases abruptly for these sizes, and they are too small to be detected by the sizing laser that triggers the ablation laser. Particles are sized by passing between two laser beams; they are then desorbed and ionised by a Nd:YAG laser. An electric field is applied to the ions, separating them by charge and causing them to pass into two separate mass spectrometers. For each data set about 20 runs were undertaken

For the experiment with biomass proxies, a diffusion flame supported on a wick burner was used as before [11] to generate particles of soot for comparison purposes. In this case, particle sizes were determined by diluting sampled flame gases and analysing using an electrical mobility instrument (DMS 500, Cambustion Ltd, Cambridge). The range that could be studied by this instrument was 5 to 2500 nm. Samples were collected directly from the flame using a glass probe connected to a Teflon tube. They were then introduced to the DMS via a heated sample line. A dilution factor of 5:1 was achieved using a supply of pure compressed air.

3. Experimental Results.

3.1 Composition of particles

Typical positive and negative ion mass spectra of particles from both combustion phases, flaming and smouldering, of both woods are shown in Fig. 2 and representative peaks are listed in Table 1.

Table 1 and Figure 2 here

In general, there is greater similarity between the spectra of the same combustion phase from different types of woods than between spectra of different phases of the same wood. This arises from the fact that the combustion in the flaming stage is dominated by the combustion of volatile species whilst the smouldering phase is dominated by the combustion of the wood char. There are few peaks with m/z greater than 100 because the combustion process is greatly diluted by excess air therefore diminishing the amount of organic species produced. In addition fragmentation occurs, some of which is attributed, according to Ferge et al [14] to the effect of potassium which skews the spectra. Potassium is present in the woods and is released in approximately equal amounts in the devolatilisation and smouldering stages [11]. The most intense peak in the positive ion spectra is in all cases +39, corresponding to both a potassium isotope as well as propargyl ($C_3H_3^+$).

Although complicated by possible interferences from organic ions, probable peak assignments given in Table 1 to inorganic ions based on isotope ratios can be made: K^+, $Ca^{\pm}$ and Cl^-. These are expected to influence organic constituents through catalytic action. Other inorganic ions, which play a part in the atmospheric chemistry of aerosols derived from biomass combustion and that are present with higher intensity in the MS in the flaming phase, are HSO_4^- and CN^- . The higher temperatures generated during flaming combustion of wood result in volatilisation of ash components and hence greater concentrations of inorganic species.

Parallel processes of hydrocarbon fragmentation and soot precursor synthesis produce a mixture of organic ions in the mass spectrometer. Fragmentation of the ions deriving from soot precursors such as polynuclear aromatic hydrocarbons (PAH) makes it difficult to infer information on the mechanism of soot formation, except to recognise (see Table 1) a number of peaks attributable to species characteristic of low-MW HACA intermediates. Thus the peak at +39 can be assigned at least in part to $C_3H_3^+$, a PAH fragment and again a HACA precursor. Other hydrocarbon ions, such as $C_3H_4^+$are also prominent in the spectra from both willow and softwood. We have previously shown [11] how soot formation from eugenol can proceed via a route involving cyclopentadienyl; the first stages of this could also be evident in wood combustion through combination of propargyl with acetylene.

Emissions from both woods also gave peaks corresponding to fragments of oxygen containing aliphatic molecules (eg. m/z=-41, C_2HO^-) consistent with the large number of oxygenated compounds in chromatograms of the products of pyrolysis and combustion of

softwood (pine) observed in our previous work [4]. A major oxygen – containing species in both willow and softwood soot spectra correspond to a peak at m/z -59 previously [7,8] used to distinguish levoglucosan and sugars from eugenol. Fig. 3 shows the contrast between the spectra obtained here for wood and the mass spectrum obtained via the same technique for soot from a eugenol flame.

Figure 3

3.2 Determination of EC/TC ratio

The ATOFMS measure the amount of elemental carbon (EC), which is effectively the same as Black Carbon (which is measured optically hence the different terminology), and Total Carbon (TC). The difference between Total Carbon and Elemental Carbon is the Organic Carbon (OC). The EC is measured in these experiments by the mass spectrometric determination of a number of C_n^- (n=2-4) species, and TC is derived from the peaks originating from organic compounds. The dimensionless ratio of elemental carbon (EC) to total carbon (TC) of the particles was determined by the method of Ferge et al. [14]. These were found to be soft wood: flaming 61±7% and smouldering 62±3%; and willow flaming 50±10% and smouldering 65±4%. A statistical t-test revealed that the willow flaming and smouldering values differed significantly, whereas for softwood combustion EC/TC for the two phases were not significantly different. This is presumably because once the biomass has been completely devolatilised to form char the difference between the wood chars is small. The values given here are upper values because of an instrumental factor that is the energy used in the ablation laser was slightly over the value recommended by Ferge et al [14].

3.3 Determination of particle diameters

Fig. 4 shows the particles size distribution from SRC willow flaming combustion. Data was also obtained from smouldering combustion which is not shown. In both cases there is a distribution of particles between 180- 350 nm with a maximum at about 280 nm. In the case of flaming combustion there are a small number of particles up to 2 µm. In the smouldering phase there is qualitative evidence that there are particles present with diameters of 50-60 nm. These particles can only be due to evaporated metallic aerosols such as potassium salts and this has been observed by other researchers [10, 12, 13]. In addition there is a greater concentration of particles in the 1 to 2.5 µm region than for flaming combustion for both

softwood and SRC willow. The particle concentrations are larger from smouldering combustion presumably from the combined effects of the ash and the fragmentation of the char as it burns out.

Figure 4 here

The size distribution for flaming combustion is similar to those produced by burning pure eugenol or furfural. Eugenol is produced by the thermal decomposition of the lignin in the wood and furfural is produced by the cellulose. Fig, 5 shows the aerodynamic diameter distributions of eugenol soot and furfural soot about 4cm above the flame. The flame varies slightly in height so a series of measurements were made over a short period of time to check that there was little variation. It is clear that eugenol flame produces more soot than the furfural flame.

Fig. 6 shows aerodynamic diameter distributions of eugenol and furfural soot but sampled further up the combustion chamber (8cm). The particles have agglomerated at this stage and larger particles are observed, with significant amounts up to 0.2 μm. This effect is larger for the soot particles from the eugenol flame because of the higher soot concentrations.

Figures 5 and 6

The type of ATOFMS used in this study does not give particle sizes below 100nm. In order to validate the general nature of the experimental results observed here additional measurements were made using an electrical mobility instrument (DMS). Figure 7 shows results obtained by DMS from the flame tip and shows significant amounts of particles about 50nm diameter but with agglomerated particles above 1 μm. This is consistent with the data in Figs 5 and 6.

Figure 7

4. Discussion

Black carbon plays an important role in atmospheric chemistry [2]. The relative proportions of elemental and co-emitted organic carbon measured by the ratio EC/TC are vital in the modelling of climate forcing. In this work, the measured EC/TC values were similar to that of soot in a road tunnel [14], namely 50.6% using the same technique. Little information is

available using this single particle technique for wood combustion but a number of measurements have been made using gravimetric filtration method. Thus Orasche et al [7] studied a number of woods burning under efficient combustion conditions using a continuously fed furnace using this and obtained much lower values.[14]. The EC/TC behaviour for the different wood samples and combustion phases in this work was similar, but a statistical t-test revealed that the willow flaming and smouldering values of ET/TC differed significantly, whereas for softwood combustion EC/TC for the two phases did not, presumably because at this stage the main process is the combustion of char.

The variation with particle size is significant because smaller particles are breathed more deeply into the lungs. Most particles studied in this work had diameter less than 2.5 μm with the greatest concentration at <0.12 μm. The similarity between ET/TC for the combustion of wood observed here to the value previously observed [11] for eugenol (52±6%) is consistent with its use as a proxy for a both hard and soft wood combustion. Interestingly it is less than that for the hydrocarbon fuel n-decane (88±5%). Further, the fraction of the total carbon emitted as elemental carbon provides important information on the consequences for the chemistry of the atmosphere of the open burning of biomass, both burning and smouldering, to yield black carbon which influences the main climate forcing terms: the solar absorption influence on liquid and ice clouds; and deposition on snow and ice [2].

The average aerodynamic diameter of all detected particles was determined for both combustion phases of willow. A distribution of sizes with average and error (defined as two standard deviations) was determined and 0.57± 0.06 μm for the flaming phase and as 0.62±0.04 um for the smouldering phase. These values have limited value and are only useful as an indication that smouldering phase particles are larger on average than those from the flaming phase. However, in confirmation, a statistical test revealed that the smouldering and flaming phase data came from different populations. Similar conclusions were drawn from particle-size data for the combustion phases of softwood where the average particle diameters were 0.68± 0.08 um (smouldering phase) and 0.58±0.05 (flaming phase). Moreover particles of this size have higher cloud nucleation efficiency while the presence of oxygen in many high intensity peaks may indicate that the aerosol particles are more hydrophilic, and therefore more active as cloud condensation nuclei, in comparison with particles from hydrocarbon products.

The correlation of a number of particle properties with the burning phase was investigated. Previous studies have suggested that sodium and potassium emissions are higher in the flaming phase of combustion. However, in this work the ratio of intensities of the +39 and +41 peaks for particles from both burning phases from both woods differed significantly from the known potassium isotopic ratio due to the interference of $C_3H_3^+$ at +39; nor did the intensity of the sodium +23 peak correlate with the combustion phase. Chlorine has been shown to play a key role in particle formation but the concentration is small here and it was concluded that chlorine could not be used to distinguish between smouldering and flaming phases but is absent from the combustion emissions of both types of wood studied here. The concentration of chlorine is low in these fuels and the potassium compounds formed are KOH and the dimer both stable at these temperatures.

Implications of this work for stove technology are the significant difference between the emissions in the flaming and smouldering phases of combustion of wood. Whilst the emissions from both hardwood and softwood were similar in the smouldering phase there were significant differences between the two types of wood in the flaming phase.

5. Conclusions

1. Representative samples of wood (softwood mix, and short-rotation willow) commonly used as fuels were burned under conditions which allowed separation of the flaming and smouldering stages of wood combustion. Emitted particles were analysed by atmospheric time of flight mass spectrometry and details of their composition determined.

2. Previous work in which the decomposition products of proxy compounds of wood (eugenol and furfural) were demonstrated to be relevant for improving our understanding of the combustion of actual wood.

3. Mass spectra of the particles from wood combustion suggest the presence of soot precursors.

4. EC/TC ratios for short-rotation willow, softwood and eugenol were similar but less than the same ratio for n-decane.

5. Potassium and chloride contents could not be used to differentiate between the phases of combustion, but particle diameter exhibited small but statistically significant differences.

6. Implications for health were that the diameters of most of the particles were less than 2.5µm and that the particle size varied with composition.

7. The implications for atmospheric chemistry included the measured particle size distribution which showed the greatest concentration of particles were <0.12 µm. Oxygen was present in many mass spectrometric peaks.

Acknowledgement

We wish to acknowledge support from the EPSRC Bioenergy Hub research programme and also thank Professor Alison Tomlin for the use of the DMS instrument.

References

1. A. K. Bolling, J. Pagels, K.E. Yttri, L. Barregard, G.Sallsten, P.E. Schwarze, C. Boman, Health effects of residential wood smoke particles: the importance of combustion conditions and physicochemical particle properties, Particle and Fibre Toxicology 6 (2009) 29.
2. T.C. Bond, S.J. Doherty, D.W. Fahey, P. Forster, T. Berntsen et al., Bounding the role of black carbon in the climate system. A scientific assessment, J. Geophys. Res: Atmos. 118 (2013) 5380-5552.
3. T. Nussbaumer, C. Czasch, N. Klippel, L. Johansson, C. Tullin, Particulate Emissions from Biomass Combustion in IEA Countries. Survey on Measurements and Emission Factors IEA Bioenergy Task 32 Zurich, (2008) ISBN 3-908705-18-5, www.ieabcc.nl
4. E.M. Fitzpatrick, J.M. Jones, M. Pourkashanian, A.B. Ross, A. Williams, K.D. Bartle, Mechanistic Aspects of Soot Formation from the Combustion of Pine Wood, Energy Fuels 22 (2008) 3771–3778.
5. E.M. Fitzpatrick, K.D. Bartle, M.I. Kubachi, J.M. Jones, M. Pourkashanian, A.B. Ross, A. Williams, K. Kubica, The mechanism of the formation of soot and other pollutants during the co-firing of coal and pine wood in a fixed-bed combustor, Fuel 88 (2009) 2409–2417.
6. T. Lee, A.P. Sullivan, L. Mack, J.L.Jimenez, S.M. Kreidenweis et al., Chemical smoke marker emissions during flaming and smouldering phases of laboratory open burning of wildland fuels, Aerosol Science and Technology 44 (2010) i–v.
7. J. Orasche, J. Schnelle-Kreis, C. Schön, H. Hartmann, H. Ruppert, J.M. Arteaga-Salas, R. Zimmermann, Comparison of emissions from wood combustion Part 2. Impact of combustion conditions on emission factors and characteristics of particle-

bound organic species and PAH-related toxicological potential, Energy Fuels 27 (2013) 1482−1491.

8. M. Elasser, C. Busch, J. Orasche, C. Schon, H. Hartmann, J. Schnelle-Kreis, R. Zimmermann R, Dynamic changes of the aerosol composition and concentration during different burning phases of wood combustion, Energy Fuels 27 (2013) 4959-4968.

9. J. Pagels, D.D. Dutcher, M.R. Stolzenburg, P.H. McMurry, M.E. Galli, D.S. Gross, Fine-particle emission from solid combustion studied with single-particle spectrometry: Identification of markers for organics, soot and ash components, J Geophys. Res. Atmos.118 (2013) 859-870.

10. T. Torvela, J. Tissari, A. Viren, K. Kaivosoja, A. Vien, A. Lahde, J. Jokiniema. Effect of wood combustion conditions on the morphology of freshly emitted fine particles. Atmos Environment, 87(2014) 65-75.

11. J.M. Wilson, M.T. Baeza-Romero, J.M. Jones, M. Pourkashanian, A. Williams, A. R. Lea-Langton, A.B. Ross, K.D. Bartle, Soot formation from the combustion of biomass pyrolysis products and a hydrocarbon fuel, n-decane: an ATOFMS study, Energy Fuels 27 (2013) 1668−1678.

12. J.M. Jones, L.I. Darvell, T.G. Bridgeman, M. Pourkashanian, A. Williams, An investigation of the thermal and catalytic behaviour of potassium in biomass combustion, Proc. of the Combust. Inst., 31 (2007) 1955-196.

13. S.C. Van Lith, P.A. Jensen, F. Frandsen, P. Glarborg, Release to the gas phase of inorganic elements during wood combustion part 2. Influence of fuel composition, Energy Fuels 22 (2008) 1598-1609.

14. T. Ferge, E. Karg, A. Schroppel, K.R. Coffee, H.J. Tobias, M. Frank, E.E. Gard, R. Zimmermann, Fast determination of the relative elemental and organic carbon content of aerosol samples by on-line single- particle aerosol time-of-flight mass spectrometry, Environ. Sci. Technol. 40 (2006) 3327-3335.

TABLE 1. Peak Assignments used for interpretation of ATOFMS data

Hydrocarbons		**Oxygen containing ions**		**Inorganic ions**	
-24	C_2^-	-41	C_2HO^-	-26	CN^-
-25	C_2H^-	+43	$C_2H_3O^+$	+27	Al^+
-26	C_2H_2		CH_3CO^+	+37 -37	Cl^+ Cl^-
+27	$C_2H_3^+$	-59	$CH_3CO_2^-$	+39	K^+
-36	C_3^-		$C_2H_3O_2^-$	+40	Ca^+
+38	$C_3H_2^+$		$C_2H_6CHO^-$	+41	K^+
+39	C_3H_3+			+56	KOH^+
+40	$C_3H_4^+$				
+41	$C_3H_5^+$				
-48	C_4^-				
+50	$C_4H_2^+$				
+51	$C_4H_3^+$				
+77	$C_6H_5^+$				

Figure Legends

Figure 1. Schematic of the experimental setup and (a) flaming combustion phase, (b) end of flaming stage/ start of smouldering combustion.

Figure 2. Example positive and negative spectra for SRC willow and softwood flaming and smouldering phase datasets. Top Left: SRC willow smouldering phase. Bottom Left: SRC willow flaming phase. Top Right: Softwood smouldering phase. Bottom Right: Softwood flaming phase.

Figure 3. Normalized positive-ion MS of eugenol soot at five laser desorption ionization (LDI) laser power densities. Reprinted from J.M. Wilson et al., Energy Fuels 27 (2013) 1668−1678. Copyright (2013) American Chemical Society.

Figure 4. Particles size distribution from SRC Willow at flaming combustion

Figure 5. Aerodynamic diameter distributions of soot produced by combustion of the proxy fuels sampled from Port 1(just above the flame): (a) eugenol and (b) furfural soot. The times represent the time after the flame has been ignited.

Figure 6. Aerodynamic diameter distributions of soot produced by combustion of the proxy fuels sampled from Port 4 well above the flame: (a) eugenol and (b) furfural soot. The times represent the time after the flame has been ignited.

Figure 7. Particle sizes of soot produced by combustion of eugenol on a wick burner obtained using DMS-represents flaming combustion

Figures

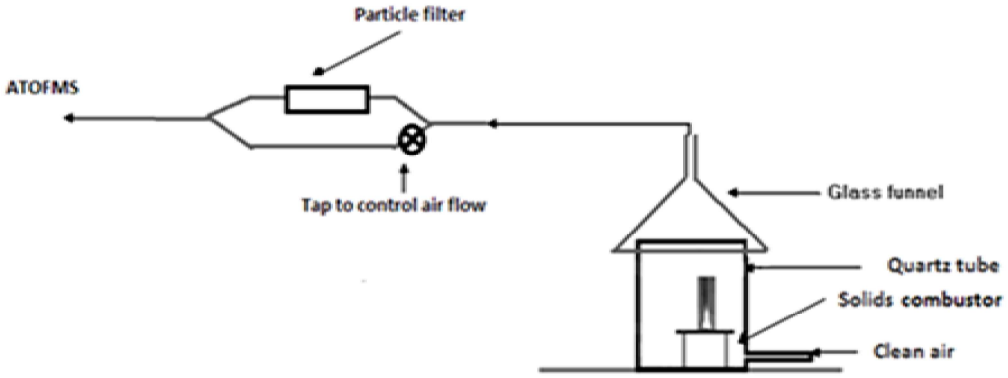

a)

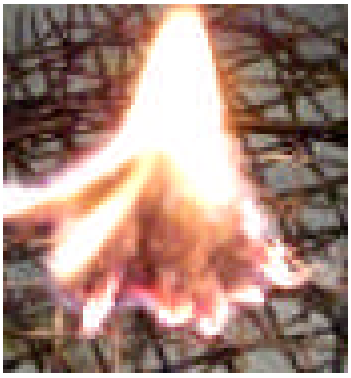

b)

Figure 1. Schematic of the experimental setup and (a) flaming combustion phase, (b) end of flaming stage/ start of smouldering combustion.

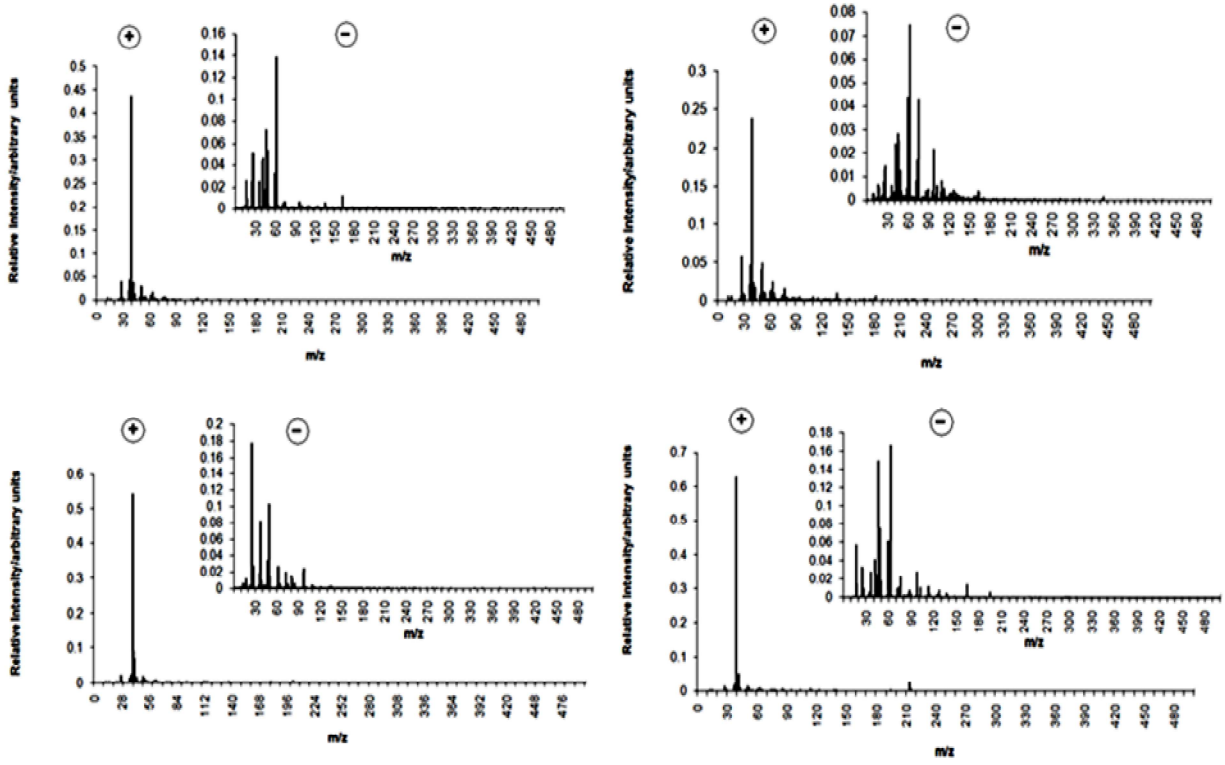

Figure 2. Example positive and negative spectra for SRC willow and softwood flaming and smouldering phase datasets. Top Left: SRC willow smouldering phase. Bottom Left: SRC willow flaming phase. Top Right: Softwood smouldering phase. Bottom Right: softwood, flaming phase.

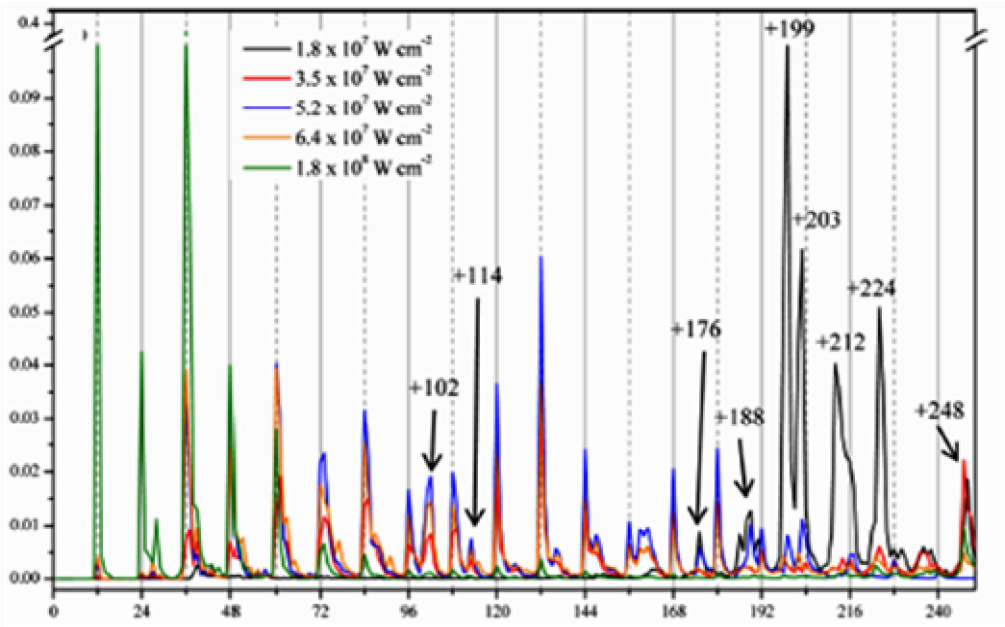

Figure 3. Normalized positive-ion MS of eugenol soot at five laser desorption ionization (LDI) laser power densities. Reprinted from J.M. Wilson et al., Energy Fuels 27 (2013) 1668−1678. Copyright (2013) American Chemical Society.

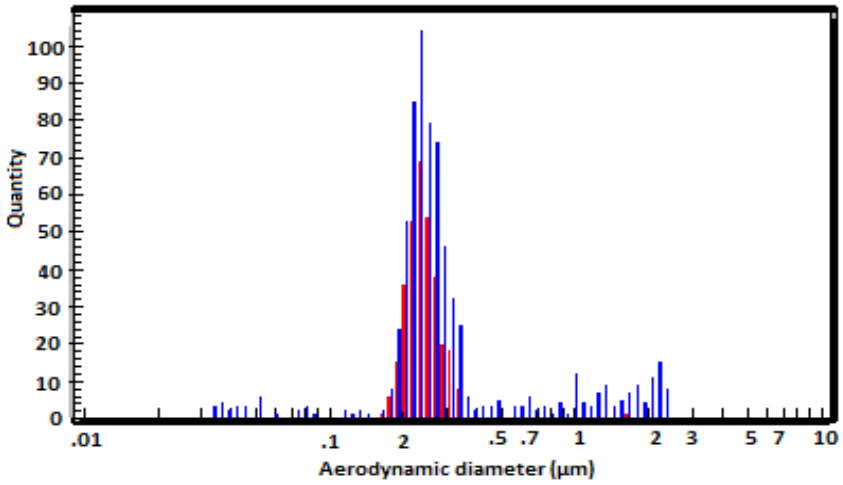

Figure 4. Particles size distribution from SRC Willow: flaming combustion

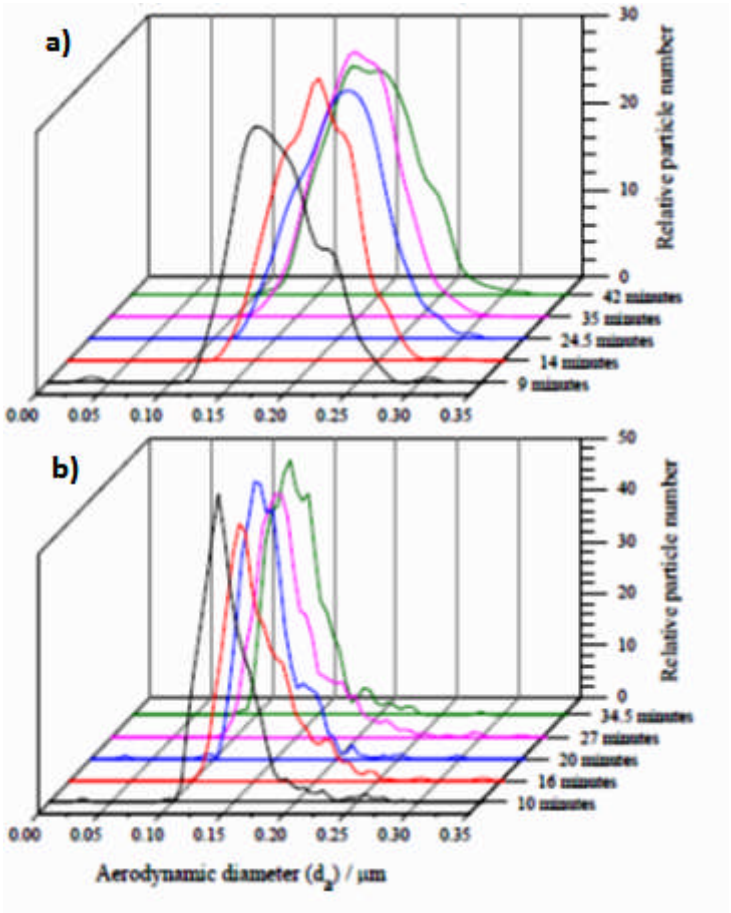

Figure 5. Aerodynamic diameter distributions of soot produced by combustion of the proxy fuels sampled 4 cm above the flame: (a) eugenol and (b) furfural soot. The times represent the time after the flame has been ignited.

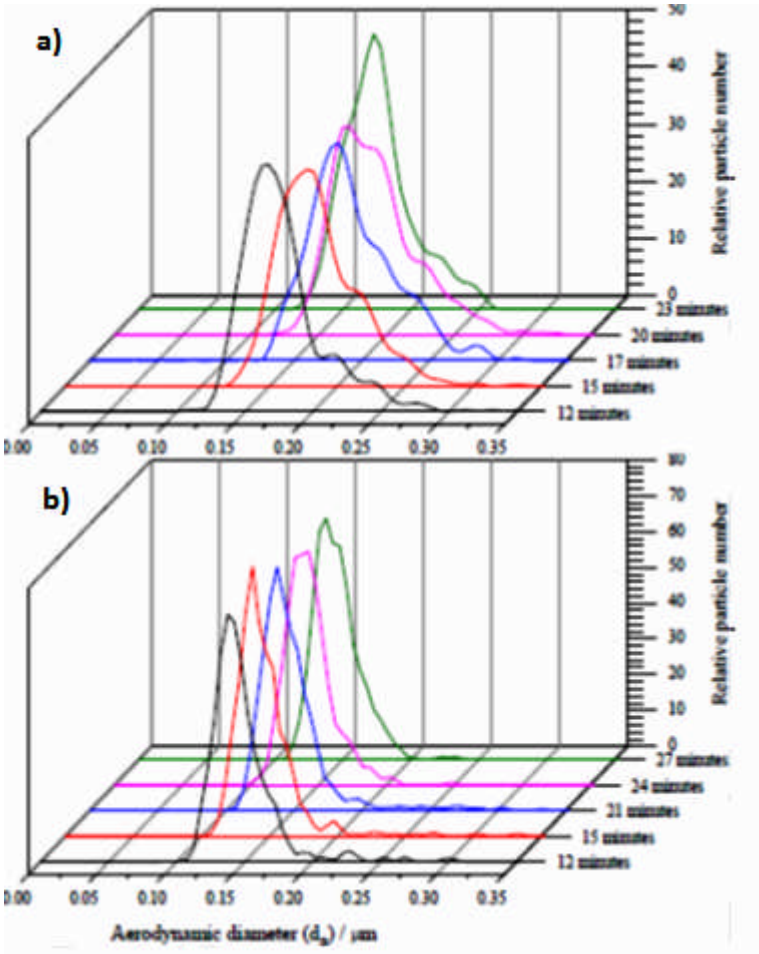

Figure 6. Aerodynamic diameter distributions of soot produced by combustion of the proxy fuels sampled 8cm above the flame: (a) eugenol and (b) furfural soot. The times represent the time after the flame has been ignited.

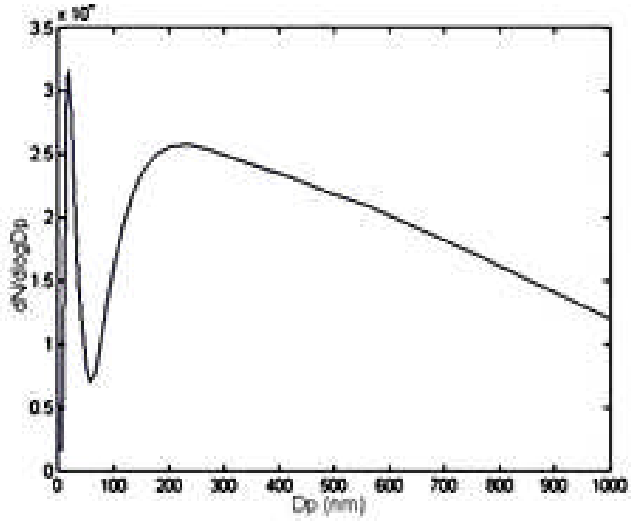

Figure 7. Particle sizes of soot produced by combustion of eugenol on a wick burner obtained using DMS-represents flaming combustion